



Effect of Electrostatic Field Assisted Thawing on the Quality of Previously Frozen Beef Striploins

Grace E. Corrette¹, Haley J. Jeneske¹, Linnea A. Rimmer¹, Larissa A. Koulicoff¹, Sara Hene¹, Morgan D. Zumbaugh¹, Travis G. O'Quinn¹, Scott Eilert², Bret Flanders³, and Michael D. Chao^{1*}

¹Department of Animal Sciences and Industry, Kansas State University, Manhattan, KS 66506, USA

²Cargill Innovations Center, Wichita, KS 67202, USA

³Department of Physics, Kansas State University, Manhattan, KS 66506, USA

*Corresponding author. Email: mdchao@ksu.edu (Michael D. Chao)

Abstract: The objective of this study was to evaluate the impact of applying electrostatic field (EF)-assisted thawing on the quality attributes of previously frozen beef striploin. Beef striploins from both sides of 12 USDA Choice carcasses were halved, frozen at -40°C , and thawed under 4 EF voltage treatments: 0 kV (control), 2.5 kV, 5 kV, and 10 kV. After reaching the internal temperature of -1°C , striploins were weighed for yield calculation, swabbed for microbial analysis, fabricated into steaks, and assigned to either 0- or 14-d aging period and retail displayed for 0 or 7 d. Subjective and objective color measurements were taken during the retail display. Upon completion of retail display, Warner-Bratzler shear force (WBSF), cook loss, sarcomere length, troponin-T degradation, muscle fiber spacing, lipid oxidation, antioxidant capacity, pH, and proximate analysis were performed. All EF treatments increased purge loss compared to the control ($P < 0.05$) and did not improve thawing speed, with samples from 10 kV actually taking the longest to thaw ($P < 0.05$). The 2.5 kV and 5 kV samples aged 14 d showed less discoloration than those from 0 kV and 10 kV, and 5 kV samples aged 14 d had higher a^* than those from the other treatments ($P < 0.05$). Samples thawed under 10 kV showed a reduction in WBSF compared to the control ($P < 0.05$), but there was no impact of EF on aerobic plate count, sarcomere length, troponin-T degradation, relative fat %, crude protein %, moisture %, purge protein concentration, pH, lipid oxidation, or antioxidant capacity for either the hydrophilic (water soluble) and lipophilic (lipid soluble) portion of the samples ($P > 0.05$). Overall, our study determined that there was no economic benefit to apply EF during thawing regarding yield and purge loss. However, the application of EF may improve tenderness and extend shelf life of beef during retail display.

Key words: beef, discoloration, electrostatic field, frozen, tenderness, thawing

Meat and Muscle Biology 8(1): 17199, 1–16 (2024)

doi:10.22175/mmb.17199

Submitted 1 December 2023

Accepted 16 February 2024

Introduction

Freezing is a cold-chain management method that is widely practiced by the meat industry to extend the shelf life of beef products (Kim et al., 2015). This extension of shelf life from freezing can reduce losses due to spoilage as well as maintain a steady supply of beef for the consumers when there is a disruption in the supply chain (Heinz and Hautzinger, 2007). Unfortunately, the process of freezing and thawing of beef can result in increased purge loss and additional discoloration during retail display due to

damage to the muscle cell membrane caused by ice crystal formation (Leygonie et al., 2012; Watanabe et al., 2018). Therefore, frozen beef products are often viewed as inferior to fresh, never frozen beef (Grunert et al., 2004). However, there are ways to mitigate the ice crystal damage of frozen products from proper thawing techniques. For example, thawing beef at a low and steady temperature can avoid recrystallization, the phenomenon of water molecules reforming into larger and irregular-shaped ice crystals when frozen meat is exposed to fluctuating temperatures (Vicent et al., 2019). As a result, there is motivation

from the meat industry to investigate new ways to thaw beef products that may reduce the negative impacts of freezing.

One of the novel technologies aiming to improve frozen food quality is known as electrostatic field (EF)-assisted thawing, which was first developed by Ohtsuki (1991) with the goal to mitigate thawing losses and decrease thawing time. The EF technology relies upon applying a high voltage output and a low alternating current (AC) to frozen food products over the entirety of thawing time. The concept is that the EF AC can cause rapid ion oscillation in the ice crystals and resulting in increased energy dissipation and heat transfer (Wei et al., 2008), which may decrease thawing time. Other studies have shown that this rapid ion oscillation of the ice crystals over time may result in the larger ice crystals breaking apart into smaller, more uniform ice crystals (Rahbari et al., 2018), which may potentially reduce cell membrane damage.

EF thawing has been investigated and has displayed the potential economic incentive to decrease purge loss and increase thawing rates. It was observed by Qian et al. (2019) that applying a voltage at 2.5 kV to frozen beef striploins shortened thawing time by 42% and reduced purge loss by approximately 20%. This finding was also observed by Jia et al. (2017), who applied EF at 20 kV to frozen rabbit meat and showed that the thawing time was shortened by 60% and purge loss decreased by 30%. The EF-assisted thawing has also demonstrated the ability to improve quality characteristics, such as reducing lipid oxidation in rabbit meat (Jia et al., 2017) and decreasing microbial loads in pork tenderloins (He et al., 2013). However, none of these studies were conducted in a standard industry operating environment, in which full-size beef subprimals are thawed in a cooler at $\sim 2^{\circ}\text{C}$. Therefore, the objective of this study was to characterize the effects of EF-assisted thawing on beef quality attributes during subsequent aging and retail display.

Materials and Methods

Sample collection and preparation

The EF thawing system consists of a high voltage power supply equipped with a voltage controller (NDT-10KV, New Defrost Technology Inc., Taipei, Taiwan), a thawing cart consists of stainless-steel meat trays placed on a stainless-steel meat cart with rubber insulations beneath each of the 4 wheels of the meat cart and a power cable that connects the alternating

signal from the high voltage power supply to the meat cart (Figure 1). The voltage signal of the high voltage power supply alternates with respect to the building ground. The voltage applied to the system was verified using a multimeter (177, Fluke Corp., Everett, WA) connected to a high voltage probe (80K-40, Fluke Corp.). It is important to note that the voltages were only verified for the carts, not for the products being thawed.

Twelve USDA Choice beef carcasses were selected from a commercial processing facility in Nebraska. Striploins (*longissimus lumborum*) from both sides of each carcass were collected at 2 d postmortem, vacuum-packaged, and transported to the Kansas State University meat lab. The next day (3 d postmortem), the purge was collected aseptically from each vacuum package, and an area approximately 10 cm \times 10 cm on the ventral side of the striploin was swabbed using a 3M Sponge Stick with 10 mL neutralizing buffer (3M Microbiology, St. Paul, MN). Following the swabbing, each striploin was portioned into 2 equal parts to result in 4 equal portions of striploin from each carcass ($n = 48$), and each portion was vacuum-packaged. A Q series 4.5-in penetration probe (THS-113-615, ThermoWorks Inc., American Fork, UT) was inserted into the geometric center of each portion through the vacuum package,



Figure 1. A representative image of the experiment setup using the electrostatic thawing system that consists of the electrostatic field generator (red arrow) and a stainless-steel meat cart (black arrow).

and the strip loin portions were frozen at -40°C without vacuum for at least 14 d. The 4 striploin portions from the same carcass were assigned to 1 of the 4 EF thawing treatments: 0 kV, 2.5 kV, 5 kV, or 10 kV in a saturated arrangement of the 4 portions to minimize any location effect within each muscle. Each voltage treatment was repeated 4 times over 4 thawing periods in the carcass cooler (0°C to 2°C). There was a total of 4 carts utilized in each thawing period, with each cart representing one specific voltage treatment. Internal temperatures of all portions were recorded throughout the thawing process using a temperature logger (THS-291-401, ThermoWorks Inc.). The thawing process was considered complete when the core temperature of all striploin portions reached at least -1°C .

After thawing, striploin portions were swabbed on the ventral side at another $\sim 10\text{ cm} \times 10\text{ cm}$ area that was not previously swabbed (3M Sponge Stick with 10 mL neutralizing buffer, 3M Microbiology) and weighed. Purge was also collected aseptically for microbial and protein concentration analysis. Each striploin portion was fabricated into four 2.54-cm steaks and five 1.27-cm steaks. One 1.27-cm steak was immediately utilized for histological analysis. The 2.54-cm steaks and remaining four 1.27-cm steaks were vacuum-packaged and assigned to either 0 or 14 d of additional aging post-thawing. After completion of the designated aging periods, steaks were overwrapped with polyvinyl chloride (23,250 cc/m²/24 h at 23°C and 0% relative humidity; Sysco, Houston, TX) in Styrofoam trays (17S; Genpak, Charlotte, NC) lined with a tray absorbent pad (Dri-Loc AC25; Novipax, Oak Brook, IL) and placed in a coffin-style retail display case (model DMF8; Tyler Refrigeration Corp., Niles, MI) under fluorescent lighting (32 W Del-Warm White 3,000 K; Phillips Lighting Company, Somerset NJ) averaging $2,143 \pm 113\text{ lx}$ emission across the case. All steaks were designated for 0- or 7-d retail display periods.

Discoloration and objective color measurements

Discoloration of each steak was evaluated daily by 6 trained panelists consisting of meat science faculty and graduate students. Panelists were trained prior to panels to evaluate and distinguish the forms of myoglobin, with discoloration being defined as the deoxy- and oxy-myoglobin pigment transitioned to metmyoglobin. Discoloration was scored by each panelist on a scale of 0 (no discoloration was present) to 100 (the steak was completely discolored). Objective color measurements were collected according to American Meat Science

Association (AMSA) Meat Color Measurement Guidelines as described in King et al. (2023). Readings for L^* , a^* , and b^* were collected 6 times on each steak using a HunterLab Miniscan EZ spectrophotometer (Illuminant D65, 2.54-cm-diameter aperture, 10° observer; Hunter Associates Laboratory, Reston, VA) during each day of retail display (0 to 7 d). The spectrophotometer was calibrated prior to use each day using a standardized white and black tile. Throughout the retail display periods, steaks were randomly rotated to various locations in the case every 24 h to ensure balanced intensity for light and temperature. The average temperature of the cases was 3°C , with 2 defrost cycles occurring at midnight and noon each day for 30 min. After completion of the designated aging and display periods, the 2.54-cm steaks designated for Warner-Bratzler shear force (WBSF) were vacuum-packaged and stored at -20°C until further analysis. The 1.27-cm steaks designated for lab analysis were frozen in liquid nitrogen, pulverized with commercial blenders (model 51BL32, Waring Commercial, Torrington, CT), and stored at -80°C until further analysis.

Microbial analysis

Swabs and purge were collected from striploin portions both before thawing to establish a baseline microbial concentration and after thawing (before retail display) to assess effects of EF on microbial reduction. Neutralizing buffer was squeezed out of the sponges from the swabs and was serially diluted to 1, 1/10, and 1/100 in a neutral phosphate-buffered saline (PBS) using aseptic techniques. The collected purge was also serially diluted following the same procedure. Following serial dilutions, 1 mL of each dilution was plated in duplicate on 3M Aerobic Plate Count (APC) petrifilm plates (3M Microbiology). The APC plates were incubated at $37^{\circ}\text{C} \pm 2^{\circ}\text{C}$ for $48 \pm 2\text{ h}$. Per the 3M Petrifilm Interpretation Guide for Aerobic Count Plates, all red colonies grown were counted and recorded.

Histological analysis for muscle fiber spacing

The one 1.27-cm steak designated for histological analysis was immediately cored after fabrication (before retail display). Three $1\text{ cm} \times 1\text{ cm} \times 1\text{ cm}$ muscle cores were collected from each steak parallel to the muscle fiber direction. Cores were suspended in optimal cutting temperature medium (Thermo Fisher, Hampton, NH) in $22\text{ mm} \times 22\text{ mm} \times 20\text{ mm}$ Epremedia plastic embedding molds (Thermo Fisher) and immediately frozen in liquid nitrogen cooled isopentane.

Frozen cores in embedding molds were stored at -80°C until further analysis.

Frozen cores were cut perpendicular to the muscle fiber direction using a microtome cryostat (Microm HM 550; Thermo Fisher) to a thickness of $20\ \mu\text{m}$ at -20°C and adhered onto a positively charged microscope slide (Globe Scientific, Mahwah, NJ). Following slicing, slides were allowed to dry and equilibrate to room temperature for 15 min before being stained in 1% hematoxylin for 5 min, rinsed in slow-running deionized water for 5 min, and submerged in 50% eosin for 2 s, 50% ethanol for 10 s, 70% ethanol for 10 s, 95% ethanol for 30 s, and a final fixative step of 100% ethanol for 30 s. Finally, slides were completely submerged in xylene for 1 s for 7 times and sealed with EpreDia Shandon-Mount (Thermo Fisher) with a coverslip placed over top and allowed to dry for 30 min before imaging. Slides were imaged using a $20\times$ objective lens on a Nikon Eclipse Ti2 inverted microscope (Nikon Instruments, Tokyo, Japan), and images were captured using a Nikon DS-Fi3 camera through NIS-Elements software (Nikon Instruments). Imaging software ImageJ (v. 1.53, U.S. National Institutes of Health, Bethesda, MD) was used to measure the distance between the sarcolemma of one muscle cell to the adjacent one in micrometers. Thirty measurements were collected from each core, for a total of 90 measurements for each sample. The mean of the 90 measurements was reported as the muscle fiber spacing for each sample.

Warner-Bratzler shear force

The WBSF was conducted on samples following the retail display. The steaks were prepared following the AMSA Research Guidelines for cookery and evaluation (AMSA, 2016). Steaks were thawed at $2^{\circ}\text{C} \pm 2^{\circ}\text{C}$ for 24 h prior to cooking, and steaks were weighed prior to cooking. Steaks were grilled on a Cuisinart Griddler Deluxe Clamshell (Cuisinart, Stamford, CT) to an internal temperature of 71°C measured by a thermometer with a metal needle inserted into the geometric center of each steak (Thermopen MK4; Thermoworks, American Fork, UT). Temperatures were monitored, and peak temperature and cooked weight of each steak were recorded. Cooked steaks were allowed to cool at $2^{\circ}\text{C} \pm 2^{\circ}\text{C}$ for 24 h. Six 1.27-cm-diameter cylinder samples from each cooled steak were taken parallel to the muscle fiber direction and sheared perpendicular to the muscle fiber orientation using a V-shaped WBSF blade attachment (G-R Elec. Mfg., Manhattan, KS) coupled to an Instron Universal Testing System (Model 5569; Instron Corporation, Norwood, MA)

set at a speed of 250 mm/min. The mean shear force (kilogram) values of the 6 cores were calculated for each steak.

Purge protein concentration

One milliliter of purge collected post-thawing (before retail display) was diluted to a 1:100 ratio in 0.1M Tris-HCl, 1.25 mM ethylenediaminetetraacetic acid (EDTA), 2% sodium dodecyl sulfate (SDS) buffer. Protein concentration (mg/mL) was determined utilizing a Pierce BCA Protein Assay Kit (Thermo Fisher) following manufacturer's guidelines.

Troponin-T degradation

Troponin-T degradation was analyzed on samples following the retail display using methods described in Hammond et al. (2022) with modification. Approximately 0.2 g of pulverized samples were weighed into tubes containing prefilled 3 mm zirconium beads and 1 mL of ice-cold ultrapure water. Samples were homogenized for 30 s using a bead homogenizer (Bead Blaster 24; Benchmark Scientific, Sayreville, NJ) and transferred to a 1.5 mL microcentrifuge tube. Samples were centrifuged at $4,000 \times g$ for 5 min. The supernatant was decanted, and the pellet was resuspended in 1 mL of ice-cold ultrapure water and recentrifuged. This process was repeated 2 more times to remove as much sarcoplasmic protein as possible. The remaining pellet was resuspended in 1 mL of extraction buffer consisting of 0.1M Tris-HCl, 1.25 mM EDTA, and 2% SDS buffer. Samples were vortexed thoroughly, centrifuged at $4,000 \times g$ for 5 min, and the supernatant was removed as final protein stock. Protein stock concentration was determined utilizing a Pierce BCA Protein Assay Kit (Thermo Fisher) following manufacturer's guidelines. Protein stock concentration of each sample was adjusted to $2,000\ \mu\text{g}/\text{mL}$ before further analysis.

Myofibrillar proteins from each sample was combined with Laemmli SDS sample buffer with reducing agent (J63615; Alfa Aesar, Haverhill, MA) at 1:1 ratio and was heated on a heat block for 95°C for 5 min. At each gel, 5 μL of Fisher Bioreagents protein ladder (Thermo Fisher) was loaded into the first lane of the gel for reference. Following the protein ladder, 5 μg of myofibrillar protein was loaded into the remaining wells of a 10% tris-glycine gel (XP00100PK2; Invitrogen, Carlsbad, CA) and run using a Mini Gel Tank (Invitrogen) filled with ice-cold tris-glycine SDS running buffer at a constant voltage of 180 V for 50 min. Following gel electrophoresis, the proteins were transferred to a polyvinylidene fluoride membrane using

an iBlot 2 gel transfer device (Invitrogen) with settings of 20 V for 1 min, 23 V for 4 min, and 25 V for 2 min. All membranes were blocked for 60 min with OneBlock Western-FL Blocking Buffer (Genesee Scientific, San Diego, CA). After blocking, 10 mL of the anti-troponin-T mouse monoclonal primary antibody (JLT-12, MilliporeSigma, Burlington, MA) at 1:2,000 dilution in blocking buffer was added to membranes and incubated at room temperature for 1 h. Following primary antibody incubation, 3 washes with 1X Tris buffered saline with tween-20 (TBST) at 5 min each were conducted on each membrane. Following the wash, 10 mL of secondary antibody (anti-mouse IgG Alexa Fluor Plus 488; A32723; Invitrogen) at 1:5,000 dilution in blocking buffer was added and incubated for 1 h at room temperature. Following secondary antibody incubation, 3 washes with 1X TBS-T and 1 final wash of 1X TBS at 5 min each were conducted. The membrane was imaged using the iBright Imaging System (FL1500, Thermo Fisher) with the Alexa Fluor 488 setting (excitation: 455 to 485 nm and emission: 508 to 557 nm) and analyzed using iBright Analysis Software (Thermo Fisher). Troponin-T degradation was determined by dividing the band intensity of the identified degraded bands by the intensity of all identified troponin-T bands within the same lane and was reported as a relative percentage.

Sarcomere length

Sarcomere length was assessed on samples prior to retail display using the methods described by Hammond et al. (2022). A few speckles of pulverized sample were sprinkled onto a charged slide (Globe Scientific) and allowed to dry for 10 min. A hydrophobic pen (Daido Sangyo Co., Tokyo, Japan) was used to make a border around the spread sample. Two hundred and fifty microliters of monoclonal anti- α -actinin anti-mouse primary antibody (Sigma-Aldrich, St. Louis, MO) at 1:5,000 dilution in 10% horse serum/0.2% Triton-X was added to each slide and incubated overnight in a humidified box. The following day, the primary antibody was removed, and the slides were rinsed 3 times with a 1X PBS solution for 5 min per rinse. Following rinsing, 250 μ L of goat anti-mouse IgG Alexa Fluor Plus 488 (A32723; Invitrogen) secondary antibody at a 1:1,000 dilution in 10% horse serum/0.2% Triton-X was added and incubated for 30 min in a humidified box. Slides were protected from light at all steps following secondary antibody incubation. After incubation, the secondary antibody was removed, and slides were rinsed 3 times with a 1X PBS solution for 5 min per rinse. After rinsing, 5 to 6 drops of 9:1

glycerol/PBS solution were added to the slide and a coverslip was placed on top of the slide and lightly pressed down. The coverslip was sealed with clear nail polish and allowed to dry. Slides were imaged using a 100 \times oil-emersion objective lens on the enhanced green fluorescent protein wavelength filter and captured using a Nikon DS-QiMc camera (Nikon Instruments) on a Nikon Eclipse Ti2 microscope (Nikon Instruments) through NIS-Element. A total of 3 images were imaged for each sample. Again, ImageJ (v. 1.53, U.S. National Institutes of Health) was used to measure the distance of a minimum of 30 sarcomeres per sample, and the 30 measurements were averaged for each sample.

Lipid oxidation

The extent of lipid oxidation was assessed on samples after retail display using the thiobarbituric acid (TBA) reactive substances assay as described in Dahmer et al. (2022). For analysis, approximately 0.2 g of the pulverized samples was weighed and recorded in prefilled bead tubes with exact weights recorded, and 1 mL of trichloroacetic acid (TCA)/TBA (20% w/v TCA: 15% w/v TBA) and 50 μ L of 3% butylated hydroxytoluene in ethanol was added. Samples were homogenized for 45 s using a bead homogenizer (Bead Blaster 24; Benchmark Scientific, Sayreville, NJ) and centrifuged at 2,000 \times g for 5 min. Supernatant was transferred into a 12 \times 75 mm glass tube. The samples were incubated at 70°C in a water bath for 30 min followed by an ice-cold water bath for 5 min. Two hundred microliters of each sample were pipetted in duplicate in a 96-well microplate. A standard curve containing 0 to 25 μ M of malondialdehyde (MDA) was also plated to be used for the calculation of sample MDA concentration. Plates were then read in a spectrophotometer at a wavelength of 532 nm (Eon; BioTek Instruments Inc., Winooski, VT) to determine MDA concentration. The sample MDA concentration was recorded as milligrams of MDA/kg of meat.

pH analysis

The pH analysis was conducted on samples prior to retail display based on the method described by Hammond et al. (2022). Five grams of pulverized muscle sample was weighed into 100 mL glass beakers. Fifty milliliters of ultrapure water was added to each sample and homogenized for 20 s at 10,000 rpm using a bench top homogenizer with a medium probe (Homogenizer 850, Thermo Fisher).

An InLab Science Pro-ISM probe connected to a Seven Compact pH meter (Meter Toledo; Columbus, OH) was calibrated using pH 4.0 and 7.0 standard solutions prior to pH measurement. The ultimate pH of each sample was measured by placing the probe into sample homogenate under constant stirring using a magnetic stirrer.

Proximate analysis

Moisture analysis was determined on samples prior to retail display by methods outlined in a modified 950.46 AOAC oven-drying method (AOAC International, 2000a). Briefly, aluminum pans were pre-labeled and dried at 110°C for 30 min in a forced air oven (Isotemp, Thermo Fisher, Pittsburgh, PA). Following drying, aluminum pans were weighed, and 5 g of pulverized sample were weighed into the aluminum pans and dried in the oven for 24 h. Samples were cooled in a desiccator for at least 30 min, after which the final weights were recorded. Moisture percentage was calculated by the initial sample weight minus the final (dried) weight, divided by the initial weight, and multiplied by 100.

Crude protein was determined on samples prior to retail display according to a modified AOAC method 992.15 (AOAC International, 2000b). Approximately 0.5 g of pulverized sample were loaded into ceramic crucibles with exact weights recorded. Ceramic crucibles were loaded into a TruMac N (LECO Corporation, St. Joseph, MO) following calibration with EDTA standards. Percent crude protein was calculated by multiplying percent nitrogen by the factor of 6.25.

Lipid content was quantified on samples prior to retail display using the method described by Folch et al. (1957) with modifications. Glass tubes were pre-labeled and dried in a forced air oven (Isotemp, Thermo Fisher) set at 100°C for 30 min prior to sample being added. The weight of the pre-labeled and predried tubes was recorded. Half a gram of pulverized sample was weighed into a 15 mL polypropylene conical tube with exact weights recorded. Following weighing, 1.5 mL of ultrapure water, 4 mL of chloroform, and 4 mL of methanol were added to the sample. Samples were shaken for 10 min using a Wrist Action Shaker (Model; 75 Burrel Corporation, Pittsburgh, PA). Following the shaking, 2 mL of 0.74% potassium chloride solution was added and thoroughly vortexed, then samples were centrifuged at 1,000 × *g* for 5 min. One milliliter of chloroform was extracted from the bottom layer with care to not disturb the meat and top layer and transferred into the predried 16 × 100 mm glass tubes.

Chloroform was evaporated using a nitrogen evaporator (REACTI-VAP III #TS-18826, Thermo Fisher). Test tubes were transferred back into the oven set to 100°C for 30 min to remove excess moisture. Percent fat was calculated by dividing the calculated lipid weight (difference of final weight and glass tube) by the mass of meat (in grams) and multiplying by 100.

Oxygen radical absorbance capacity

The oxygen radical absorbance capacity (ORAC) procedure was performed on samples after retail display according to methods described by Chun et al. (2023). For the lipophilic portion, 1 mL of hexane was added to 0.1 g of pulverized sample in pre-filled bead tubes. Samples were homogenized for 45 s in the bead homogenizer and shaken for 1 h at room temperature. After shaking, samples were centrifuged at 3,000 × *g* for 10 min, and the hexane layer was collected and evaporated under nitrogen. Seven hundred fifty microliters of 7% randomly methylated beta-cyclodextrin in 50:50; acetone:water was added to redissolve the lipophilic portion. For hydrophilic portion, 1 mL of 80% water:20% ethanol solution was added to the same tube and homogenized for an additional 45 s in the bead homogenizer. Samples were centrifuged at 12,000 × *g* for 10 min. Seven hundred and fifty microliters of supernatant was collected for analysis. Both lipophilic and hydrophilic portions were stored at –80°C until further analysis.

Prior to sample and standard addition to the plate, 150 µL of working solution consisting of 4 µM of sodium fluorescein in 75 mM phosphate buffer was added to all wells of a black 96-well plate (3631; Corning, Corning, NY). Hydrophilic portions were further diluted 1:20 with 80% water:20% ethanol solution, and the lipophilic portions were not diluted prior to being added to the plate. Twenty-five microliters of sample was added in triplicates, and the plates were incubated at 37°C for 30 min. After incubation, 25 µL of 2,2'-azobis (2-amidinopropane) dihydrochloride solution was added to each well to initiate the reaction. A multi-mode plate microplate reader (Synergy HTX; BioTek Instruments Inc.) was used with fluorescence filters for an excitation wavelength of 485 nm and an emission wavelength of 528 nm. Fluorescence of each well was measured from the bottom every 60 s for 120 min for a total of 120 measurements. The ORAC values were measured as the net area under the curve (AUC). The net AUC is calculated by subtracting the AUC of the samples from the AUC of the blank. A standard curve was obtained by plotting Trolox

concentrations (0 to 100 μM) against their average net AUC for the hydrophilic and lipophilic portions. The final unit was calculated as micromole of Trolox equivalent per gram of meat.

Statistical analysis

Data were analyzed using the PROC GLIMMIX procedure of SAS (v. 9.4, SAS Institute, Cary, NC). Thawing time, purge loss, purge protein concentration, proximate analysis, pH analysis, sarcomere length, and muscle fiber spacing were analyzed as a randomized complete block design, with each thawing period serving as the block. The microbial analysis was analyzed as one-way analysis of covariance with the fixed effect as the EF treatments and the initial microbial load as the covariate. Cooking loss, WBSF, troponin-T degradation, lipid oxidation, and ORAC were analyzed as a split-split plot where the whole plot is the EF treatments, the subplot is the post-thawing aging period, and the sub-subplot is the retail display days. Finally, subjective and objective meat color data were analyzed as a split-split-plot repeated-measures design with EF treatments as the whole plot, post-thawing aging period

as the subplot, and retail display day as the repeated-measures. The experimental unit was each meat cart ($n = 16$; 4 per treatment). The Toeplitz covariance structure was selected because it had the smallest value for Akaike’s information criterion. Multiple comparisons were obtained through Tukey method, and mean separation was conducted using least-squares mean procedures. Differences among means were detected at $P < 0.05$ level using the least significant difference.

Results and Discussion

Purge loss, thawing time, and cook loss

There was a treatment effect for purge loss, in which the purge loss for the 5 and 10 kV EF treatment samples was greater than those from 0 kV ($P < 0.05$; Table 1). However, the purge loss for 2.5 kV treatment was not different than those from any other EF treatments ($P > 0.05$). There were no differences among the treatments in thawing time from -35°C to -5°C ($P > 0.05$; Figure 2). However, there was a treatment effect in thawing time from -5°C to -1°C , where

Table 1. Main effect of treatment for purge loss, cook loss, aerobic plate counts (APC), proximate analysis, pH, sarcomere length, muscle fiber spacing, troponin-T degradation, Warner-Bratzler shear force (WBSF), lipid oxidation, and oxygen radical absorbance capacity (ORAC) of beef striploins thawed under different electrostatic field treatments

Treatments	0 kV	2.5 kV	5 kV	10 kV	SEM ⁴	P Value
Purge Loss (%)	1.36 ^b	1.72 ^{ab}	1.94 ^a	2.20 ^a	0.22	<0.05
Cook Loss (%)	15.76	15.91	16.62	16.33	0.50	0.51
APC-Swab (log CFU/mL)	2.32	2.30	2.20	2.41	0.08	0.10
APC-Purge (log CFU/mL)	2.19	2.08	1.90	2.11	0.11	0.50
Moisture %	70.37	70.46	70.64	70.16	0.43	0.74
Protein %	22.30	22.26	22.42	22.11	0.18	0.45
Fat %	6.50	6.53	6.35	6.84	0.49	0.80
pH	5.67	5.64	5.65	5.65	0.02	0.34
Purge Protein Concentration (mg/mL)	52.49	51.20	49.82	47.20	2.24	0.37
Sarcomere Length (μm)	2.01	1.92	1.89	1.96	0.05	0.17
Muscle Fiber Spacing (μm)	11.25	9.53	10.17	11.47	0.84	0.09
Troponin-T Degradation ¹ (%)	88.91	90.00	88.32	89.92	2.03	0.54
WBSF (kgf)	3.33 ^{ab}	3.21 ^{bc}	3.39 ^a	3.13 ^c	0.15	<0.05
Lipid Oxidation (mg of MDA ² /kg of Meat)	0.28	0.26	0.26	0.26	0.05	0.98
Hydrophilic ORAC (TE ³ /g of Meat)	17.06	16.30	16.23	17.18	0.63	0.33
Lipophilic ORAC (TE/g of Meat)	0.33	0.31	0.30	0.31	0.02	0.75

^{a-c}Least-squares means within a row without common superscript differ; $P < 0.05$.

¹Relative percentage of degraded troponin-T.

²MDA = malondialdehyde.

³TE = Trolox equivalent.

⁴Standard error of least-squares means.

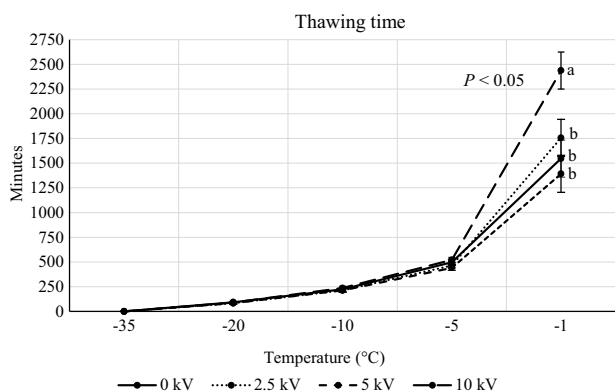


Figure 2. Time (minutes) it takes for striploin halves from each of electrostatic field treatments to reach -20°C , -10°C , -5°C , and -1°C . ^{a,b}Least-squares means within a temperature without common superscript differ; $P < 0.05$.

the 10 kV treatment samples took longer to reach -1°C than any of the other treatments ($P < 0.05$). For cooking loss measurement, there was no 3-way interaction among treatment \times aging \times display or 2-way interaction between treatment \times aging ($P > 0.10$). However, there was a tendency for treatment \times display interaction for cook loss ($P = 0.08$). Overall, all EF samples that were displayed for 7 d had less moisture loss during the cooking process than those from samples aged for 0 d, except for those from the 10 kV EF-treated samples ($P = 0.08$; data not shown).

Qian et al. (2019) determined that beef striploin thawed under the application of 2.5 kV EF had less purge loss compared to those thawed at room temperature. Furthermore, Jia et al. (2017) observed that applying 20 to 25 kV to frozen rabbit meat during thawing can improve water-holding capacity compared to those from lower voltage treatments of 15 and 0 kV. However, our study observed contrasting results from those reported by others, where both 5 and 10 kV EF samples actually had increased purge loss compared to the control in this study. It is interesting to note that all of our samples thawed equally until -5°C with no purge loss, after which heavy purge loss was observed. Water phase change temperature in meat is between -1°C and -7°C (Belozarov et al., 2020). It was generally thought that the longer the product stayed at this temperature, the greater damage would occur due to repeated recrystallization (Vicent et al., 2019), resulting in more muscle damage in these samples and loss of more free water as purge.

Mousakhani-Ganjeh et al. (2016b) thawed frozen tuna fish with EF voltage ranging from 0 kV to 14 kV, where they observed increased voltages were directly proportional to increased thawing speeds. This finding was further confirmed by Jia et al.

(2017), who applied EF voltages ranging from 0 kV to 25 kV to frozen rabbit meat and observed that the thawing rate increased up to 60% with increased voltage. This noted improvement in thawing time observed in other studies has again been attributed to the notion that the ionic movement under the influence of EF can increase friction and heat transfer in meat (Rahbari et al., 2018). While these studies all demonstrated that voltage increase reduces thawing times, our results contrasted with these findings as we have shown that the frozen striploins from the 10 kV treatment actually had the longest thawing time. Costa et al. (1999) observed that the loss of free water can negatively impact the heat transfer in potatoes. We hypothesize that all water was still in its frozen state until melting began at around -5°C . Beyond that point, our most intense EF treatments drove the most intense ionic motions in the liquid fractions of the thawing samples (Fagan et al., 2005; Lu et al., 2022), resulting in protein denaturation due to the dissipated heat. Perhaps the increased purge loss from the higher voltage treated samples negatively affected the thawing speed due to a reduction in heat transfer coefficient from increased purge loss noted earlier.

Mousakhani-Ganjeh et al. (2015) thawed frozen tuna fish with EF voltage ranging from 0 to 14 kV and observed that all EF treatments increased cooking loss. Additionally, Rahbari et al. (2018) thawed frozen chicken breast under EF voltages ranging from 0 to 18 kV and observed that EF applications regardless of voltage increased cooking loss. However, Hsieh et al. (2010) observed no thawing loss or cook loss difference while thawing frozen chicken breast at 20 kV compared to conventional thawing at -3°C . In our study, the 10 kV samples displayed for 7 d tended to have greater cooking loss compared to those from the control and the 2.5 kV treatment, which again demonstrated that application of high voltage EF may reduce water-holding capacity. It is important to note that this is the first known study that utilized frozen striploin halves (~ 2.7 kg) under EF thawing, while the other previously mentioned studies looked at small pieces of individual muscles. As meat freezes, its internal water content solidifies and limits the movement of ions, thus altering its conductivity (Marra, 2013). The striploin portions used in this study, being larger pieces of meat, would require a significantly longer time to reach the same level of conductivity as smaller pieces due to the prolonged thawing process. Therefore, it is possible that the difference of sample size could explain some of the differing findings of EF applications from other studies compared to those from our study.

Microbial analysis

There was no treatment effect for the swab or purge APC data ($P > 0.05$; Table 1). He et al. (2013) observed that pork tenderloin decreased in total microbial counts when thawed under 4 to 10 kV EF treatments, and Zhang et al. (2023) reported that the application of 3 kV EF reduced total viable cell count in large yellow croaker fish compared to those that received no EF treatment. Wu et al. (2022) further confirmed this antimicrobial effect by investigating *Escherichia coli* O157:H7 survival rate in apple juice that was treated with 0.8 kV EF, where they noted that EF caused irreversible cell membrane ruptures in the cells and ultimately resulting in cell death and reduction of total viable cell counts. However, our findings are not consistent with the previously mentioned studies in showing consistent reduction of total APC. Hsieh et al. (2010) also observed no increase in total viable counts for chicken meat thawed at -3°C . The cooler temperatures in our study ranged from 0°C to 2°C , and the final internal temperature of each striploin portion was around -1°C . These lower temperatures could have been the contributing factor that controlled the growth of bacteria and showed no differences in APC in our study, regardless of the voltage applied for both the external surface as well as the purge.

Proximate analysis, purge protein concentration, and pH measurements

There was no treatment effect on percentages of moisture, protein, or fat of the samples, protein concentration in the purge, or pH of the samples ($P > 0.05$, Table 1). It was expected that EF will not alternate the protein and fat content, but it was to our surprise that no EF effect was observed for moisture content as the 5 and 10 kV EF samples had statistically greater purge losses compared to those from the other treatments. However, it is important to note that the difference between these treatments was less than 1%, and that small differences can explain the lack of impact of EF treatments on total moisture content.

Qian et al. (2019) noted less protein present in the purge from beef striploin thawed under 2.5 kV EF compared to traditional thawing. The same authors hypothesized that as EF can decrease damage to the muscle cell membrane, which less sarcoplasmic cellular contents would have leaked out of the cells into the extracellular space. Additionally, Traore et al. (2012) also determined that exudate content can indicate the degree of protein denaturation and oxidation. However, our finding likely means that the EF treatments

from our study did not reduce any damage from the ice crystal formation or reduce any protein denaturation, and thus, protein concentration in the purge was not reduced from the EF applications. In fact, it is possible that samples from the EF treatments had greater damage due to heat production from the ion oscillation, which resulted in the greater purge loss, as discussed earlier. Finally, both Jia et al. (2017) and He et al. (2013) evaluated the effect of EF on pH in rabbit meat and pork loin thawed under EF, respectively, and they both observed that EF treatments had no impact on pH of thawed meat products, which agreed with our findings.

Sarcomere length, muscle fiber spacing, and troponin-T degradation

There was no treatment effect on sarcomere length ($P > 0.05$; Table 1 and Figure 3). However, there was a tendency for treatment effect on muscle fiber spacing that the 10 kV and control samples tended to have greater muscle fiber spacing compared to those from the 2.5 kV treatments, while the muscle fiber spacing was not different for the 5 kV treatment when compared to those from any of the other treatments ($P = 0.09$; Table 1 and Figure 4). There was no 3-way interaction of treatment \times aging \times display or interactions of treatment \times aging or treatment \times display for troponin-T degradation ($P > 0.05$; Figure 5). In addition, there was no main effect of treatment effect on troponin-T degradation ($P > 0.05$; Table 1). As expected, there was an aging \times display interaction ($P < 0.05$; Table 2), where samples aged for an additional 14 d and retail displayed 7 d showed the highest relative percentage of degraded troponin-T, and samples with no additional aging and retail display showed

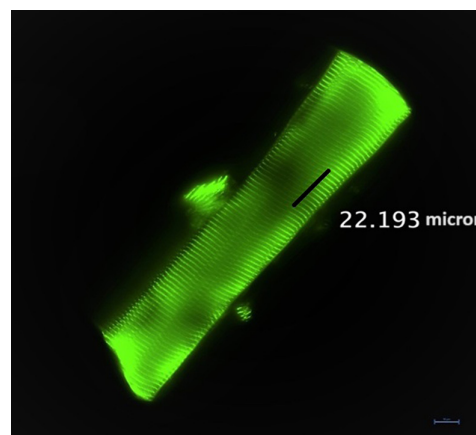
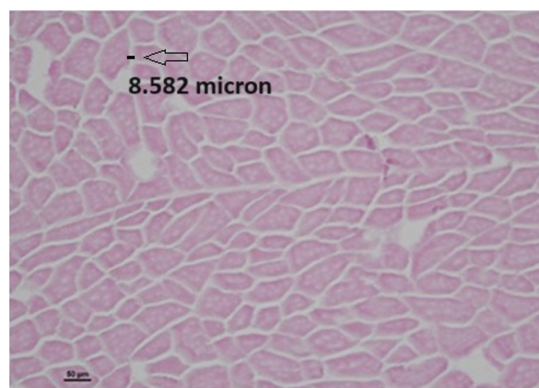
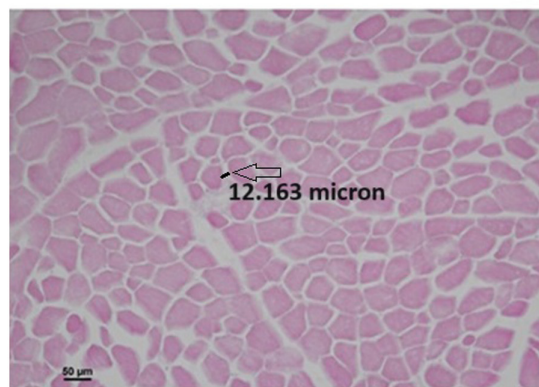


Figure 3. Representative image of sarcomere length measurement featuring 10 sarcomeres being measured (22.19 μm).



Representative image of cross section for 2.5 kV EF



Representative image of cross section for 10 kV EF

Figure 4. Representative image of muscle fiber cross sections demonstrating measurements for muscle fiber spacing from 2.5 and 10 kV electrostatic field treatments (muscle fiber: red; extracellular space: white).

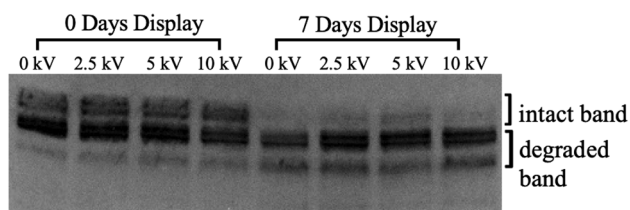


Figure 5. Representative image of troponin-T degradation featuring different display periods demonstrating intact and degraded troponin-T bands.

the lowest relative percentage of degraded troponin-T compared to all other aging and retail display periods ($P < 0.05$). Samples aged for an additional 14 d with no retail display showed no difference in troponin-T degradation with those from samples that had no additional aging but were retail displayed for 7 d ($P < 0.05$).

Zhang et al. (2017) and Qi et al. (2012) both observed that sarcomere length can be shortened after multiple cycles of freezing and thawing. While the exact nature of how the formation of ice crystals can

Table 2. Effect of aging × display interaction for Warner-Bratzler shear force (WBSF), troponin-T degradation, and hydrophilic oxygen radical absorbance capacity (ORAC) assay of beef striploins thawed under different electrostatic field treatments

Aging	Display	WBSF (kgf)	Troponin-T Degradation ¹ (%)	Hydrophilic ORAC (TE ² Equivalent/g of Meat)
0 Day of Aging	0 d	3.86 ^a	77.10 ^c	14.24 ^c
Additional Aging	7 d	3.22 ^b	91.49 ^b	15.76 ^b
14 Days of Aging	0 d	3.00 ^c	92.24 ^b	15.72 ^b
Additional Aging	7 d	2.97 ^c	96.33 ^a	21.06 ^a
	SEM ³	0.15	1.36	0.65
	<i>P</i> value	<0.05	<0.05	<0.05

^{a-c}Least-squares means within a row without common superscript differ; $P < 0.05$.

¹Relative percentage of degraded troponin-T.

²TE = Trolox equivalent.

³Standard error of least-squares means.

impact sarcomere length is not yet fully understood, the current hypothesis is that the formation of the ice crystals can cause the sarcomeres to expand. When the ice crystals melt, the sarcomeres will contract back to their original position (Qi et al., 2012). However, the repeated freeze-thaw cycle can cause extensive damage to the sarcomere and result in eventual collapse of Z-disk leading to sarcomere shortening, which Qian et al. (2019) observed that application of 2.5 kV EF while thawing beef striploin could prevent this noted shortening of sarcomeres from the repeated freeze-thaw cycle. There were no differences in sarcomere length among the treatments in our study. A possible explanation is that our study only had one freezing cycle and that the ice crystals were not allowed to reform multiple times, thus preventing the collapse of Z-disk.

Due to the characteristic of water as a dipole, it is possible that the ice crystals can break apart when an extremely impose field alternates back and forth (Mukherjee et al., 2021). Therefore, our thought process was that if EF treatments can reduce ice crystal size in the extracellular space, we should observe reduced spacing between muscle fibers. The 10 kV treatment did not reduce the spacing between muscle fibers in our study, but the 2.5 kV treatment has a tendency to have smaller muscle fiber spacing compared to the control. Qian et al. (2019) also observed that when thawing beef striploin under 2.5 kV, the EF treatment reduced the distance of the gaps between muscle fibers. Furthermore, Lung et al. (2022) observed that Peking duck thawed under pulsed electric field voltages of

1 to 3 kV had lower average distance between the muscle fibers compared to the control. However, when the same group of authors applied pulsed electric field at 4 kV to thawing duck meat, they failed to observe a decrease in distance between muscle fibers compared to those from the traditionally thawed samples (Lung et al., 2022). Van der Sman (2017) hypothesized that increasing voltage can cause additional damage to the microstructure of meat from the heat generated, resulting in increased distances between muscle fibers. Perhaps this could be used to explain why only the 2.5 kV treatment from our study had a tendency to reduce muscle fiber spacing compared to the control.

As a result of the ion movement caused by the AC of the EF, we anticipated increased protein denaturation caused by the associated energy dissipation. Mousakhani-Ganjeh et al. (2015) observed that frozen tuna fish thawed under 4.5 kV to 14 kV showed increased protein denaturation as the voltage intensity increased compared to air thawing. Calpain is a major proteolytic enzyme that can be easily denatured (Zhang and Erbjerg, 2018), and Qian et al. (2019) hypothesized that calpain activity can be inhibited by the EF. This is further supported by Ko et al. (2016), who observed that tilapia stored at refrigeration under an EF of 3 kV to 9 kV showed delayed enzymatic activity, which included calpain activity. However, EF did not decrease calpain activity in our study as no difference was found in troponin-T degradation between the EF-treated samples and the control. These conflicting findings warrant further investigation on the impacts of an EF on the enzymatic activity of calpains and how this can impact the degradation of myofibrillar proteins.

Discoloration evaluation

There was a 3-way interaction among treatment \times aging \times display for the discoloration evaluated by the trained panelists ($P < 0.05$; Figure 6). Overall, there was an anticipated impact on discoloration as samples progressed during display ($P < 0.05$). For samples with no additional aging, there was no significant difference in discoloration among the treatments till day 6 of retail display. The 5 kV-treated samples showed more discoloration on day 6 and 7 of retail display compared to samples from the rest of the treatments ($P < 0.05$).

For samples aged for an additional 14 d, the increased aging time resulted in much greater overall discoloration compared to those with no additional aging ($P < 0.05$). There was no significant difference in discoloration among the aged treatments until day 3 of retail display. On day 3, 4, and 5, the 0 and

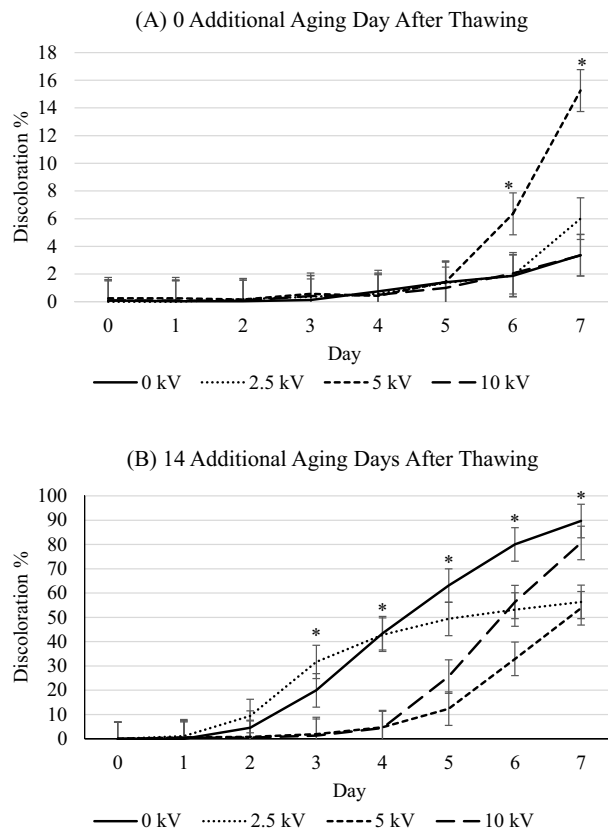


Figure 6. Discoloration % of samples from the electrostatic field thawing treatments during 7 d of retail display for (A) samples with 0 additional aging days and (B) samples with 14 additional aging days after thawing. *Days there were significant differences in discoloration % ($P < 0.05$).

2.5 kV samples were more discolored than the 5 and 10 kV samples ($P < 0.05$). The treatments showed the most variability on day 6, with 0 kV samples having more discoloration than 2.5 and 10 kV, and 5 kV had the least discoloration compared to all other EF treatments ($P < 0.05$). The 0 and 10 kV samples showed more discoloration on day 7 of retail display compared to 2.5 and 5 kV samples ($P < 0.05$).

The impact of EF showed varying impacts on color stability during thawing. Ko et al. (2016) assessed the freshness of whole tilapia fish stored at refrigeration temperatures under EF ranging from 3 to 9 kV and observed that samples treated with 9 kV EF took longer to emit a spoiled odor to trained panelists, and all EF treatments improved the brightness of the belly appearance compared to those from the control. Zhang et al. (2023) also observed that yellow croaker fish stored partially frozen under a 3 kV EF showed increased freshness characteristics such as odor, gill color, eyeball appearance, and surface color when compared to the control. These studies indicate that application of EF has the potential to preserve the appearance of freshness for various animal proteins.

Objective color evaluation

There was no 3-way interaction of treatment \times display \times aging, and there was no treatment \times display or treatment \times aging interactions for L^* values ($P > 0.05$). Finally, there was no main effect of treatment for L^* values ($P > 0.05$). There was no 3-way interaction of treatment \times aging \times display for a^* values ($P > 0.05$), but there was an interaction of treatment \times aging ($P < 0.05$; Figure 7A). For samples aged 0 d, there was no impact of treatments on a^* values ($P > 0.05$). For samples aged 14 d, the 5 kV samples had the higher a^* values than all other EF treatments ($P < 0.05$), followed by 2.5 and 10 kV samples having lower a^* values than 5 kV ($P < 0.05$), with 0 kV samples having the lowest a^* value but no different from 2.5 kV samples ($P > 0.05$).

There was also an interaction of treatment \times display for a^* values ($P < 0.05$; Figure 7B). When evaluating a^* values across display, all treatment samples displayed progressive decline of a^* values ($P < 0.05$). On day 0, all EF treatments had higher a^* compared to the 2.5 kV samples ($P < 0.05$). On days 1 to 3, 5 kV samples had greater a^* values than those from 2.5 kV ($P < 0.05$) but not different than those from the 0 and

10 kV samples ($P > 0.05$). On day 4 and 5, the 5 kV samples had higher a^* values than those from 0 and 2.5 kV samples ($P < 0.05$) but were not different to those from the 10 kV samples ($P > 0.05$). On day 6, the 5 kV-treated samples had higher a^* values than the 10 kV samples, but both the 5 and 10 kV samples were not different from the 0 and 2.5 kV samples ($P < 0.05$). All treatments reached the same a^* value on day 7 ($P > 0.05$).

There was no 3-way interaction of treatment \times aging \times display for b^* values or an interaction of treatment \times display ($P > 0.05$). However, there was an interaction for treatment \times aging for b^* values ($P < 0.05$; data not shown). For samples aged 0 days, there was no impact of treatments on b^* values ($P > 0.05$). However, when considering the samples aged 14 d, the 5 kV treatment had the highest b^* values compared to those from all other EF treatments ($P < 0.05$).

He et al. (2013) demonstrated that pork loins thawed under a 10 kV EF had greater L^* values compared to those from the control samples, but there was no impact on a^* and b^* values. On the other hand, Jia et al. (2017) showed that all EF treatments increased L^* , a^* , and b^* values of frozen rabbit meat compared to those from conventionally thawed, and as voltages increased from a range of 5 to 15 kV to 20 kV and 25 kV, the L^* and a^* values further increased. Qian et al. (2019) further showed that beef striploin treated with 2.5 kV EF improved a^* during the first 24 h of the thawing process compared to those from traditional thawing. In our study, there was no EF impact on L^* , but EF treatments improved a^* for the steaks aged 14 d, particularly for the 5 kV treatment. Along with this finding, there was a reduction in discoloration for the 2.5 kV and 5 kV EF-treated samples after 14 d of aging. In addition to this, there was an observed decrease in b^* values for samples aged for 14 d. When meat is fresher, there are higher levels of antioxidants available to maintain the redness of meat longer, which could explain why the a^* and b^* of 0 d aged samples were unaffected by the EF treatment (Echegaray et al., 2021). Maggiolino et al. (2020) observed that an increase of antioxidant status of beef ribeye could improve b^* values as well as a^* . Many forms of antioxidants such as proteins, peptides, and vitamins naturally present in muscle cells and function as color stabilizers through protecting the myoglobin from oxidation (Suman and Joseph, 2013). Joseph et al. (2012) observed that increased abundance of these color-stabilizing agents was positively correlated to increased redness in beef *longissimus lumborum*. It is possible that the application of EF can enhance the

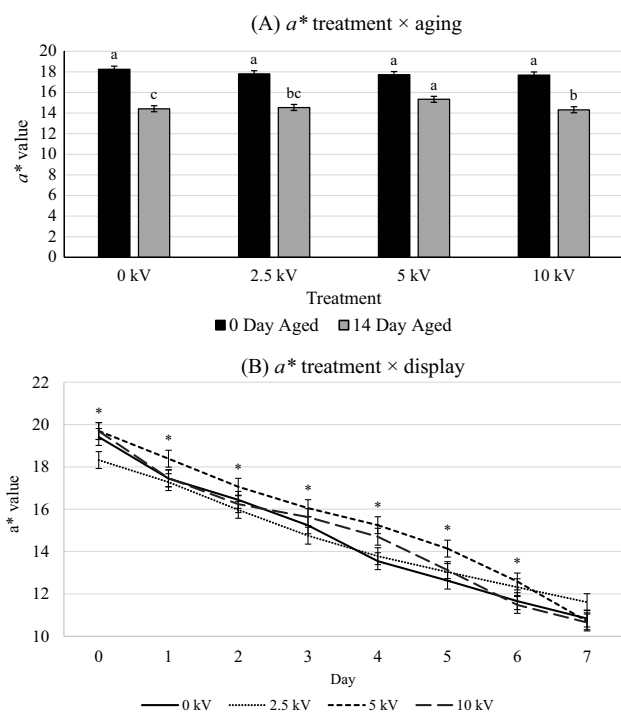


Figure 7. a^* values of samples from the electrostatic field thawing treatments for (A) 0 and 14 additional aging days after thawing regardless of display time; $^{*c}P < 0.05$ within each aging period; (B) 7 d of retail display regardless of additional aging time. *Days there were significant differences in a^* ($P < 0.05$).

activity of these antioxidants that presented in the striploins and thus led to the improvement in a^* values and prevented metmyoglobin formation.

Warner-Bratzler shear force

There was no 3-way interaction of treatment \times aging \times display or 2-way interaction of treatment \times display or interaction of treatment \times aging on WBSF ($P > 0.05$). However, there was a main effect of treatment on WBSF ($P < 0.05$; [Table 1](#)). The 10 kV samples had lower WBSF compared to those from 5 and 0 kV samples ($P < 0.05$), while WBSF from 2.5 kV samples were not different from those from the 10 kV-treated samples ($P > 0.05$). There was an expected display \times aging interaction ($P < 0.05$; [Table 2](#)). Samples aged for 0 d with no retail display had the highest WBSF compared to all other aging and retail display periods ($P < 0.05$). Samples aged for an additional 14 d had the lowest WBSF compared to samples with no additional aging regardless of retail display period ($P < 0.05$).

Qian et al. (2019) also observed a reduction in slice shear force values for beef striploin thawed under a 2.5 kV EF compared to those from traditional thawing. Although the WBSF differences among samples were miniscule, it was to our surprise that the 10 kV-treated samples had a lower shear force than all other treatments in our study. However, this improvement in tenderness in our study did not derive from the calpain system or muscle contractile status, as there were no differences in troponin-T degradation or sarcomere length among those from different EF treatments. Additionally, the 10 kV EF-treated samples did not have increased muscle fiber spacing compared to the control and 5 kV EF treatment. Qian et al. (2019) observed that the application of 2.5 kV EF decreased muscle fiber cracking, which is the phenomenon of when one muscle fiber splits into 2 in response to damage, thus requiring more force to shear through the increased number of muscle fibers and decreasing tenderness ([Barbut, 2013](#); [Chang et al., 2021](#)). The same authors hypothesized such effects may be responsible for the observed increase in tenderness ([Qian et al., 2019](#)). In addition, collagenases like matrix metalloproteinase 9 have demonstrated ability to break down connective tissue during the postmortem aging process ([Koulicoff et al., 2023](#)). Perhaps 10 kV EF has enhanced the modification of collagen structure by improving the activity of native collagenase in beef through an unknown mechanism. Further investigation looking at connective tissue structure may explain the impacts on tenderness observed in this study.

Lipid oxidation and oxygen radical absorbance capacity

There were no interactions of treatment \times aging \times display, treatment \times aging, aging \times display, or treatment \times display on lipid oxidation ($P > 0.05$). Additionally, there was no main effect of treatment or aging on lipid oxidation ($P > 0.05$; [Table 1](#)). Finally, there was a main effect of display, where there was an anticipated observed increase in lipid oxidation in samples displayed for 7 d compared to samples subjected to 0 d retail display ($P < 0.05$). When looking at the effect of EF on lipid oxidation of meat in other research, Jia et al. (2017) observed that all rabbit meat samples treated with EF, regardless of voltage intensity, showed decreased lipid oxidation values compared to those thawed without EF. However, Mousakhani-Ganjeh et al. (2016a) showed that increasing voltage showed increased lipid oxidation in frozen tuna fish during thawing. Unfortunately, we did not observe the application of EF having an impact on lipid oxidation of the samples in our study. With the noted color preservation capability from EF during retail display, it is possible that EF has the capability to reduce primary lipid oxidation products like hydroperoxide but not secondary lipid oxidation product like MDA in beef. Differences in the levels of primary and secondary oxidation products may indicate variations in the rate of oxidative processes, and analyzing both primary and secondary lipid oxidation products provides a comprehensive understanding of the oxidative status of meat during retail display ([Domínguez et al., 2019](#)). Unfortunately, only MDA, a secondary lipid oxidation product, was measured in this study.

For the hydrophilic ORAC, there was no 3-way interaction among treatment \times aging \times display or any main effect of treatment ($P > 0.05$; [Table 1](#)); however, there was an aging \times display interaction ($P < 0.05$; [Table 2](#)). Samples aged for an additional 14 d followed by 7 d display had the highest, followed by samples aged for an additional 14 d with no retail display and samples with no additional aging time with 7 d of retail display, with samples with no additional aging period or display period having the lowest Trolox equivalent/g of meat compared to those from other aging and display periods ($P < 0.05$). For lipophilic ORAC, there was no 3-way interaction among treatment \times aging \times display, aging \times display interaction, or any treatment effect ($P > 0.05$; [Table 1](#)); however, there was a main effect of aging ($P < 0.05$). Samples that were aged for an additional 14 d had higher Trolox equivalent/g of meat compared to samples with no additional aging period ($P < 0.05$; [Table 2](#)).

The ORAC method relies upon adding free radicals from the sample to the system and measures how the free radicals damage the fluorescent probes (Huang et al., 2002). The assay runs on the assumption that the greater the fluorescent intensity over time, the higher the antioxidant activity of the sample. However, the limitation with this principle is that such estimation is not the direct measurement of antioxidants present in the sample, but on oxygen free radical availability. In agreement with the lipid oxidation finding, we also observed that EF did not enhance antioxidant capacity regardless of voltages applied. This finding aligns with Sánchez-Moreno et al. (2005) who reported that application of an EF did not alter 2,2-diphenyl-1-picrylhydrazyl radical scavenging capacity in orange juice. On the other hand, our results did show that ORAC increased with aging time for both the lipophilic and hydrophilic portions, which Liu et al. (2017) also observed that as aging progressed, the ORAC gradually increased in duck meat. This likely indicated that more oxygen free radical compounds were generated over the 14 d aging time.

Conclusions and Implications

The results from this research provided valuable insight into the function of the EF and its capabilities to potentially improve frozen beef quality. Although our results showed the application of EF to beef did not improve yield or thawing time as originally expected, there were indications that this technology may improve post-thawing quality, such as tenderness and shelf stability of beef. Further investigation should look deeper into how different voltages can impact structural damage to the muscle during thawing and how the damage relates to tenderness as well as impacts on enzymatic activity.

Acknowledgements

This project was funded by National Cattlemen's Beef Association, a contractor to the Beef Checkoff.

Literature Cited

- American Meat Science Association. 2016. Research guidelines for cookery, sensory evaluation, and instrumental tenderness measurements of meat. Version 1.02. Am. Meat Sci. Assoc. Champaign, IL.
- AOAC International. 2000a. Moisture in meat. AOAC Official Method 950.46. In: W. Hoewitz, editor, Official methods of analysis of AOAC International. 17th ed. Vol. II. AOAC, Gaithersburg, MD. p. 1–2.
- AOAC International. 2000b. Crude protein in meat and meat products including pet food. AOAC Official Method 992.15. In: W. Hoewitz, editor. Official methods of analysis of AOAC International. 17th ed. Vol. II. AOAC, Gaithersburg, MD. p. 14–15.
- Barbut, S. 2013. Frying — Effect of coating on crust microstructure, color, and texture of lean meat portions. *Meat Sci.* 93:269–274. <https://doi.org/10.1016/j.meatsci.2012.09.006>
- Belozorov, A. G., Y. M. Berezovskiy, I. A. Korolev, and T. A. Sarantsev. 2020. A calculation model for the heat capacity of beef with different moisture during freezing taking into account free water crystallization. *Theory and Practice of Meat Processing* 5:29–34. <https://doi.org/10.21323/2414-438X-2020-5-4-29-34>
- Chang, L., S. Lin, B. Zou, X. Zheng, S. Zhang, and Y. Tang. 2021. Effect of frying conditions on self-heating fried Spanish mackerel quality attributes and flavor characteristics. *Foods* 10:98. <https://doi.org/10.3390/foods10010098>
- Chun, C. K. Y., M. Roth, R. Welti, M. P. Richards, W.-W. Hsu, T. O'Quinn, and M. D. Chao. 2023. Exploring the potential effect of phospholipase A2 antibody to extend beef shelf-life in a beef liposome model system. *Meat Sci.* 198:109091. <https://doi.org/10.1016/j.meatsci.2022.109091>
- Costa, R. M., F. A. R. Oliveira, O. Delaney, and V. Gekas. 1999. Analysis of the heat transfer coefficient during potato frying. *J. Food Eng.* 39:293–299. [https://doi.org/10.1016/S0260-8774\(98\)00169-1](https://doi.org/10.1016/S0260-8774(98)00169-1)
- Dahmer, P. L., F. B. McDonald, C. K. Chun, C. A. Zumbaugh, C. K. Jones, A. R. Crane, T. Kott, J. M. Lattimer, and M. D. Chao. 2022. Evaluating the impact of feeding dried distillers grains with solubles on Boer goat growth performance, meat color stability, and antioxidant capacity. *Translational Animal Science* 6:txac060. <https://doi.org/10.1093/tas/txac060>
- Domínguez, R., M. Pateiro, M. Gagaoua, F. J. Barba, W. Zhang, and J. M. Lorenzo. 2019. A comprehensive review on lipid oxidation in meat and meat products. *Antioxidants* 8:429. <https://doi.org/10.3390/antiox8100429>
- Echegaray, N., M. Pateiro, P. E. S. Munekata, J. M. Lorenzo, Z. Chabani, M. A. Farag, and R. Domínguez. 2021. Measurement of antioxidant capacity of meat and meat products: methods and applications. *Molecules* 26:3880. <https://doi.org/10.3390/molecules26133880>
- Fagan, J. A., P. J. Sides, and D. C. Prieve. 2005. Evidence of multiple electrohydrodynamic forces acting on a colloidal particle near an electrode due to an alternating current electric field. *Langmuir* 21:1784–1794. <https://doi.org/10.1021/la048076m>
- Folch, J., M. Lees, and G. H. Sloane Stanley. 1957. A simple method for the isolation and purification of total lipides from animal tissues. *J. Biol. Chem.* 226:497–509.
- Grunert, K. G., L. Bredahl, and K. Brunsø. 2004. Consumer perception of meat quality and implications for product development in the meat sector—A review. *Meat Sci.* 66:259–272. [https://doi.org/10.1016/S0309-1740\(03\)00130-X](https://doi.org/10.1016/S0309-1740(03)00130-X)
- Hammond, P. A., C. K. Y. Chun, W. J. Wu, A. A. Welter, T. G. O'Quinn, G. Magnin-Bissel, E. R. Geisbrecht, and M. D. Chao. 2022. An investigation on the influence of various

- biochemical tenderness factors on eight different bovine muscles. *Meat Muscle Biol.* 6:13902, 1–17. <https://doi.org/10.22175/mmb.13902>
- He, X., R. Liu, S. Nirasawa, D. Zheng, and H. Liu. 2013. Effect of high voltage electrostatic field treatment on thawing characteristics and post-thawing quality of frozen pork tenderloin meat. *J. Food Eng.* 115:245–250. <https://doi.org/10.1016/j.jfoodeng.2012.10.023>
- Heinz, G., and P. Hautzinger. 2007. Meat processing technology for small- to medium-scale producers. Food and Agricultural Organization of the United Nations, Regional Office for Asia and the Pacific, Bangkok, Thailand. <https://www.fao.org/documents/card/fr/c/fb92d00f-7ff3-593a-a77c-> (Accessed 1st September 2023).
- Hsieh, C. W., C. H. Lai, W. J. Ho, S. C. Huang, and W. C. Ko. 2010. Effect of thawing and cold storage on frozen chicken thigh meat quality by high-voltage electrostatic field. *J. Food Sci.* 75:193–197. <https://doi.org/10.1111/j.1750-3841.2010.01594.x>
- Huang, D., B. Ou, M. Hampsch-Woodill, J. A. Flanagan, and R. L. Prior. 2002. High-throughput assay of oxygen radical absorbance capacity (ORAC) using a multichannel liquid handling system coupled with a microplate fluorescence reader in 96-well format. *J. Agr. Food Chem.* 50:4437–4444. <https://doi.org/10.1021/jf0201529>
- Jia, G., H. Liu, S. Nirasawa, and H. Liu. 2017. Effects of high-voltage electrostatic field treatment on the thawing rate and post-thawing quality of frozen rabbit meat. *Innov. Food Sci. Emerg.* 41:348–356. <https://doi.org/10.1016/j.ifset.2017.04.011>
- Jia, G., S. Nirasawa, X. Ji, Y. Luo, and H. Liu. 2018. Physicochemical changes in myofibrillar proteins extracted from pork tenderloin thawed by a high-voltage electrostatic field. *Food Chem.* 240:910–916. <https://doi.org/10.1016/j.foodchem.2017.07.138>
- Joseph, P., S. P. Suman, G. Rentfrow, S. Li, and C. M. Beach. 2012. Proteomics of muscle-specific beef color stability. *J. Agr. Food Chem.* 60:3196–3203. <https://doi.org/10.1021/jf204188v>
- Kim, Y. H. B., C. Liesse, R. Kemp, and P. Balan. 2015. Evaluation of combined effects of ageing period and freezing rate on quality attributes of beef loins. *Meat Sci.* 110:40–45. <https://doi.org/10.1016/j.meatsci.2015.06.015>
- King, D. A., M. C. Hunt, S. Barbut, J. R. Claus, D. P. Cornforth, P. Joseph, Y. H. B. Kim, G. Lindahl, R. A. Mancini, M. N. Nair, K. J. Merok, A. Milkowski, A. Mohan, F. Pohlman, R. Ramanathan, C. R. Raines, M. Seyfert, O. Sørheim, S. P. Suman, and M. Weber. 2023. American Meat Science Association guidelines for meat color measurement. *Meat Muscle Biol.* 6:12473, 1–81. <https://doi.org/10.22175/mmb.12473>
- Ko, W.-C., H.-Z. Shi, C.-K. Chang, Y.-H. Huang, Y.-A. Chen, and C.-W. Hsieh. 2016. Effect of adjustable parallel high voltage on biochemical indicators and actomyosin Ca²⁺-ATPase from tilapia (*Oreochromis niloticus*). *LWT Food Sci. Technol.* 69:417–423. <http://doi.org/10.1016/j.lwt.2016.01.074>
- Koulicoff, L. A., T. Heilman, L. Vitanza, A. Welter, H. Jeneske, T. G. O’Quinn, S. Hansen, E. Huff-Lonergan, M. D. Schulte, and M. D. Chao. 2023. Matrix metalloproteinase-9 may contribute to collagen structure modification during postmortem aging of beef. *Meat Sci.* 205:109321. <https://doi.org/10.1016/j.meatsci.2023.109321>
- Kropf, D. 2002. Meat display lighting. PIG-12-05-03. U.S. Pork Center of Excellence, Clive, IA. <https://porkgateway.org/resource/meat-display-lighting/> (Accessed 1st August 2023.)
- Leygonie, C., T. J. Britz, and L. C. Hoffman. 2012. Impact of freezing and thawing on the quality of meat. *Meat Sci.* 91(2):93–98. <https://doi.org/10.1016/j.meatsci.2012.01.013>
- Liu, D., X. Chen, J. Huang, M. Huang, and G. Zhou. 2017. Generation of bioactive peptides from duck meat during post-mortem aging. *Food Chem.* 237:408–415. <https://doi.org/10.1016/j.foodchem.2017.05.094>
- Lu, N., J. Ma, and D.-W. Sun. 2022. Enhancing physical and chemical quality attributes of frozen meat and meat products: Mechanisms, techniques and applications. *Trends Food Sci. Tech.* 124:63–85. <https://doi.org/10.1016/j.tifs.2022.04.004>
- Lung, C.-T., C.-K. Chang, F.-C. Cheng, C.-Y. Hou, M.-H. Chen, S. P. Santoso, B. Yudhistira, and C.-W. Hsieh. 2022. Effects of pulsed electric field-assisted thawing on the characteristics and quality of Pekin duck meat. *Food Chem.* 390:133137. <https://doi.org/10.1016/j.foodchem.2022.133137>
- Maggiolino, A., J. M. Lorenzo, A. Salzano, M. Faccia, F. Blando, M. P. Serrano, M. A. Latorre, J. Quiñones, and P. De Palo. 2020. Effects of aging and dietary supplementation with polyphenols from *Pinus taeda* hydrolysed lignin on quality parameters, fatty acid profile and oxidative stability of beef. *Anim. Prod. Sci.* 60(5):713–724. <http://doi.org/10.1071/AN19215>
- Marra, F. 2013. Impact of freezing rate on electrical conductivity of produce. *SpringerPlus* 2:633. <https://doi.org/10.1186/2193-1801-2-633>
- Mousakhani-Ganjeh, A., N. Hamdami, and N. Soltanizadeh. 2015. Impact of high voltage electric field thawing on the quality of frozen tuna fish (*Thunnus albacares*). *J. Food Eng.* 156:39–44. <https://doi.org/10.1016/j.jfoodeng.2015.02.004>
- Mousakhani-Ganjeh, A., N. Hamdami, and N. Soltanizadeh. 2016a. Effect of high voltage electrostatic field thawing on the lipid oxidation of frozen tuna fish (*Thunnus albacares*). *Innov. Food Sci. Emerg.* 36:42–47. <http://doi.org/10.1016/j.ifset.2016.05.017>
- Mousakhani-Ganjeh, A., N. Hamdami, and N. Soltanizadeh. 2016b. Thawing of frozen tuna fish (*Thunnus albacares*) using still air method combined with a high voltage electrostatic field. *J. Food Eng.* 169:149–154. <http://doi.org/10.1016/j.jfoodeng.2015.08.036>
- Mukherjee, R., S. F. Ahmadi, H. Zhang, R. Qiao, and J. B. Boreyko. 2021. Electrostatic jumping of frost. *ACS Nano* 15(3):4669–4677. <https://doi.org/10.1021/acsnano.0c09153>
- Ohtsuki, T. 1991. Process for thawing foodstuffs. U.S. Patent 5,034,236. Date issued: 23 July.
- Qi, J., C. Li, Y. Chen, F. Gao, X. Xu, and G. Zhou. 2012. Changes in meat quality of ovine *longissimus dorsi* muscle in response to repeated freeze and thaw. *Meat Sci.* 92(4):619–626. <https://doi.org/10.1016/j.meatsci.2012.06.009>
- Qian, S., X. Li, H. Wang, W. Mehmood, M. Zhong, C. Zhang, and C. Blecker. 2019. Effects of low voltage electrostatic field thawing on the changes in physicochemical properties of myofibrillar proteins of bovine *Longissimus dorsi* muscle.

- J. Food Eng. 261:140–149. <https://doi.org/10.1016/j.jfoodeng.2019.06.013>
- Rahbari, M., N. Hamdami, H. Mirzaei, S. M. Jafari, M. Kashaninejad, and M. Khomeiri. 2018. Effects of high voltage electric field thawing on the characteristics of chicken breast protein. J. Food Eng. 216:98–106. <http://doi.org/10.1016/j.jfoodeng.2017.08.006>
- Sánchez-Moreno, C., L. Plaza, P. Elez-Martínez, B. De Ancos, O. Martín-Belloso, and M. P. Cano. 2005. Impact of high pressure and pulsed electric fields on bioactive compounds and antioxidant activity of orange juice in comparison with traditional thermal processing. J. Agr. Food Chem. 53(11):4403–4409. <https://doi.org/10.1021/jf048839b>
- Suman, S. P., and P. Joseph. 2013. Myoglobin chemistry and meat color. Annu. Rev. Food Sci. T. 4:79–99. <https://doi.org/10.1146/annurev-food-030212-182623>
- Traore, S., L. Aubry, P. Gatellier, W. Przybylski, D. Jaworska, K. Kajak-Siemaszko, and V. Santé-Lhoutellier. 2012. Higher drip loss is associated with protein oxidation. Meat Sci. 90(4):917–924. <https://doi.org/10.1016/j.meatsci.2011.11.033>
- Van der Sman, R. G. M. 2017. Model for electrical conductivity of muscle meat during Ohmic heating. J. Food Eng. 208:37–47. <https://doi.org/10.1016/j.jfoodeng.2017.03.029>
- Vicent, V., F. T. Ndoye, P. Verboven, B. Nicolai, and G. Alvarez. 2019. Effect of dynamic storage temperatures on the microstructure of frozen carrot imaged using X-ray micro-CT. J. Food Eng. 246:232–241. <https://doi.org/10.1016/j.jfoodeng.2018.11.015>
- Watanabe, G., M. Motoyama, I. Nakajima, and K. Sasaki. 2018. Relationship between water-holding capacity and intramuscular fat content in Japanese commercial pork loin. Asian Austral J. Anim. 31(6):914–918. <https://doi.org/10.5713/ajas.17.0640>
- Wei, S., X. Xiaobin, Z. Hong, and X. Chuanxiang. 2008. Effects of dipole polarization of water molecules on ice formation under an electrostatic field. Cryobiology 56:93–99. <https://doi.org/10.1016/j.cryobiol.2007.10.173>
- Wu, S., X. Xu, N. Yang, Y. Jin, Z. Jin, and Z. Xie. 2022. Inactivation of *Escherichia coli* O157: H7 in apple juice via induced electric field (IEF) and its bactericidal mechanism. Food Microbiol. 102:103928. <https://doi.org/10.1016/j.fm.2021.103928>
- Zhang, Y., and P. Ertbjerg. 2018. Effects of frozen-then-chilled storage on proteolytic enzyme activity and water-holding capacity of pork loin. Meat Sci. 145:375–382. <https://doi.org/10.1016/j.meatsci.2018.07.017>
- Zhang, J., L. Fei, P. Cui, N. Walayat, S. Ji, Y. Chen, F. Lyu, and Y. Ding. 2023. Effect of low voltage electrostatic field combined with partial freezing on the quality and microbial community of large yellow croaker. Food Res. Int. 169:112933. <https://doi.org/10.1016/j.foodres.2023.112933>
- Zhang, M., F. Li, X. Diao, B. Kong, and X. Xia. 2017. Moisture migration, microstructure damage and protein structure changes in porcine longissimus muscle as influenced by multiple freeze-thaw cycles. Meat Sci. 133:10–18. <https://doi.org/10.1016/j.meatsci.2017.05.019>